

# A SEMI-IMPLICIT EXPONENTIAL LOW-REGULARITY INTEGRATOR FOR THE NAVIER–STOKES EQUATIONS

BUYANG LI, SHU MA, AND KATHARINA SCHRATZ

ABSTRACT. A new type of low-regularity integrator is proposed for the Navier–Stokes equations. Unlike the other low-regularity integrators for nonlinear dispersive equations, which are all fully explicit in time, the proposed method is a semi-implicit exponential method in time in order to preserve the energy-decay structure of the Navier–Stokes equations. First-order convergence of the proposed method is established independently of the viscosity coefficient  $\mu$ , under weaker regularity conditions than other existing numerical methods, including the semi-implicit Euler method and classical exponential integrators. The proposed low-regularity integrator can be extended to full discretization with either a stabilized finite element method or a spectral collocation method in space, as illustrated in this article. Numerical results show that the proposed method is much more accurate than the semi-implicit Euler method in the viscous case  $\mu = O(1)$ , and more stable than the classical exponential integrator in the inviscid case  $\mu \rightarrow 0$ .

## 1. Introduction

This article is concerned with the numerical solution of the initial and boundary value problem of the incompressible Navier–Stokes (NS) equations

$$\begin{cases} \partial_t u + u \cdot \nabla u - \mu \Delta u + \nabla p = 0 & \text{in } \Omega \times (0, T], \\ \nabla \cdot u = 0 & \text{in } \Omega \times (0, T], \\ u = u_0 & \text{at } \Omega \times \{0\}, \end{cases} \quad (1.1)$$

in a bounded domain  $\Omega \subset \mathbb{R}^d$ , with  $d \in \{2, 3\}$ , under appropriate boundary conditions, where we have used the notation  $u \cdot \nabla u := (u \cdot \nabla)u$ . The well-posedness of the two- and three-dimensional NS equations was discussed in [7, 14, 17, 19, 23].

The NS equations are the fundamental partial differential equations describing the motion of incompressible viscous fluids. They are widely used in fluid dynamics to model water and blood flows, air flow around a wing, and ocean currents. As the exact solution is not known in most applications, the numerical solution of the NS equations plays a central role. The development of accurate, stable numerical methods, together with their rigorous error analysis, is therefore crucial and of major practical importance to reliably describe of the NS equations. Driven by the immense spectrum of applications, many different numerical methods have been proposed for solving the NS equations.

In the smooth setting, i.e., for smooth solutions and regular initial data, the numerical approximation of the NS equations is nowadays in large parts well understood and sharp rigorous global error estimates could be established; see, e.g., [11, 15, 18, 25, 26, 33, 34]. The

---

2010 *Mathematics Subject Classification.* 65M12, 65M15, 76D05.

*Key words and phrases.* Navier–Stokes equations,  $L^2$  initial data, semi-implicit Euler scheme, finite element method, error estimate.

optimal-order error estimates generally use the viscosity term to control the nonlinear term, and therefore contain a viscosity-dependent constant  $c(\mu^{-1})$  in the error bound in addition to certain Sobolev norms of the exact solution. Note that in case of large viscosity  $\mu \sim 1$  the solution of NS is regularised such that non-smooth initial data is not a big problem numerically. In particular, the rigorous error analysis of semi- and full discretisations of the NS equations with  $H^1$  initial data can be found in [12] and [9, 10, 20], respectively. This, however, drastically changes in case of small viscosity  $\mu \ll 1$ , where no smoothing can be expected and classical viscosity-dependent  $c(\mu^{-1})$  error bounds explode. Although there are explicit Runge–Kutta methods for which the stability region includes part of the imaginary axis, which would be stable in the case  $\mu \rightarrow 0$  under the stepsize condition  $\tau = o(h)$ , such methods typically require a much stronger CFL condition  $\tau = o(h^2)$  when  $\mu$  is not close to zero. Error estimates of the numerical methods for the NS equations without using the viscosity term to bound the nonlinear term (therefore robust for all range of  $\mu$ ) could recently be established for smooth solutions, see for example in [1, 3, 36]. The analysis in these articles show that the classical finite difference methods in time, such as the semi-implicit Euler method

$$\begin{cases} \frac{u_n - u_{n-1}}{\tau} + u_{n-1} \cdot \nabla u_n - \mu \Delta u_n + \nabla p_n = 0 & \text{in } \Omega \\ \nabla \cdot u_n = 0 & \text{in } \Omega \end{cases} \quad (1.2)$$

and the backward differentiation formulae, typically requires the solution to satisfy  $u \in L^\infty(0, T; H^2(\Omega)^d)$  and  $\partial_{tt}u \in L^2(0, T; L^2(\Omega)^d)$  for first-order convergence in time and space (when the error constants do not depend on the viscosity), where  $d$  denotes the dimension of space. The condition  $\partial_{tt}u \in L^2(0, T; L^2(\Omega)^d)$  actually requires  $u \in L^2(0, T; H^4(\Omega)^d)$  for the solution of the NS equations, as one time derivative of the solution is related to two spatial derivatives of the solution. As a result, the classical finite difference methods in time requires

$$u \in H^2(0, T; L^2(\Omega)^d) \cap L^2(0, T; H^4(\Omega)^d) \hookrightarrow L^\infty(0, T; H^3(\Omega)^d)$$

for first-order convergence in time and space. The analysis in the current paper further shows that the classical exponential integrators for the NS equations, such as the exponential Euler method,

$$u_n = e^{\tau_n \mu A} u_{n-1} - \int_{t_{n-1}}^{t_n} e^{(t_n-s)\mu A} P_X(u_{n-1} \cdot \nabla u_{n-1}) ds \quad \text{for } n \geq 1, \quad (1.3)$$

where  $A = P_X \Delta$  denotes the Stokes operator (with  $P_X$  being the projection onto the divergence-free subspace), would also require  $u \in L^\infty(0, T; H^3(\Omega)^d)$  for first-order convergence in time (if we require the error bound to be independent of the viscosity).

The objective of this article is to develop a new low-regularity integrator for NS which allows for first-order convergence in time and space under a weaker regularity condition  $u \in L^\infty(0, T; W^{2, d+\epsilon}(\Omega)^d)$ , where  $\epsilon$  can be arbitrarily small. In particular, we present a stabilization technique by utilizing the nonlinear convection term in the NS equations and establish global error estimates independent of  $\mu$  allowing for low-regularity approximations also in regimes of small viscosity  $\mu \ll 1$ .

Our new scheme also greatly extends previous works on low regularity integrators which mainly focus on semi-discretizations in time [30] and nonlinear dispersive equations, e.g., Schrödinger, Dirac and Korteweg-de Vries [6, 13, 27–29, 32, 38, 39]. In this work we approach the the NS equations, and, for the first time couple the idea of low regularity time discretisations

with a finite element based spatial discretisation. Note that fully discrete low regularity integrators were so far restricted to pseudo spectral methods for the spatial discretisation [22] which are not suitable for problems posed on general bounded domains. The latter are, however, especially interesting in the context of NS flow problems. The numerical experiments in this article show that the proposed low regularity integrator for the NS equations is much more accurate than the classical semi-implicit Euler method in the viscous case  $\mu = O(1)$ , and more accurate and robust than the classical exponential integrator in the inviscid case  $\mu \rightarrow 0$ . Therefore, the proposed method combines the advantages of the semi-implicit Euler method and classical exponential integrator in both viscous and inviscid cases.

The rest of this article is organized as follows. In Section 2 we construct a low-regularity integrator for the NS equations through analyzing and improving both the consistency and the stability of the classical exponential Euler method. We first present the construction of the method in the context of periodic boundary conditions and then extend it to the widely used no-slip boundary conditions in NS flow problems. The energy-decay property and error estimates of the proposed low-regularity integrator are proved for semidiscretization in time. In Section 3 we extend the low-regularity integrator to full discretization with a stabilized finite element method in space, and present error estimates for the fully discrete low-regularity integrator. Numerical examples are presented in Section 4 to compare the performance of the proposed low-regularity integrator with the performance of both the semi-implicit Euler method and the exponential Euler method. Conclusions and remarks are presented in Section 5.

## 2. The low-regularity integrator and its basic properties

In this section, we present the construction of the low-regularity integrator by analyzing the dependence of the consistency errors on the regularity of the solution. The construction is presented first for the NS equations under the periodic boundary condition in subsection 2.1 and then extended to the no-slip boundary condition in subsection 2.2.

### 2.1. Construction of the time-stepping method

In this subsection, we focus on the NS equations on the  $d$ -dimensional torus  $\Omega = [0, 1]^d$  (under the periodic boundary condition). Through integration by parts it is straightforward to verify the following property of the divergence-free subspace

$$\dot{H} := \{v \in L^2(\Omega)^d : \nabla \cdot v = 0\}.$$

If  $v \in \dot{H}$  and  $q \in H^1$  then

$$(v, \nabla q) = 0.$$

Let  $P_X : L^2(\Omega)^d \rightarrow \dot{H}$  be the  $L^2$ -orthogonal projection onto the divergence-free subspace  $X = \dot{H}$ . By using the above orthogonality, it is straightforward to verify that

$$P_X f = f - \nabla q, \tag{2.1}$$

where  $q$  is the solution (up to a constant) of the following PDE problem (under periodic boundary conditions):

$$\Delta q = \nabla \cdot f.$$

Let  $A = P_X \Delta : H^2 \rightarrow \dot{H}$ . Then the NS equations can be written as finding  $u \in C([0, T]; H^2) \cap C^1([0, T]; L^2)$  to the following problem:

$$\begin{cases} \partial_t u + P_X(u \cdot \nabla u) - \mu A u = 0 & \text{for } t \in (0, T], \\ u(0) = u_0. \end{cases} \quad (2.2)$$

From the definition of  $A$  and identity (2.1), it is easy to see that for  $f \in H^2(\Omega)^d$

$$A P_X f = P_X \Delta P_X f = P_X \Delta f - P_X \nabla \Delta q = P_X \Delta f \quad (\text{since } P_X \nabla \eta \equiv 0). \quad (2.3)$$

Moreover, if  $f \in \dot{H}^2 = \{v \in H^2(\Omega)^d : \nabla \cdot v = 0\}$  then  $\Delta f \in \dot{H}$  and therefore  $P_X \Delta f = \Delta f$ . As a result, the following identity holds:

$$A f = \Delta f \quad \text{for } f \in \dot{H}^2. \quad (2.4)$$

Let  $0 = t_0 < t_1 < \dots < t_N = T$  be a partition of the time interval  $[0, T]$  with stepsize  $\tau_n = t_n - t_{n-1}$ . According to the variation of constants formula, the solution of (2.2) satisfies the following identity:

$$u(t_n) = e^{\tau_n \mu A} u(t_{n-1}) - \int_{t_{n-1}}^{t_n} e^{(t_n-s)\mu A} P_X(u(s) \cdot \nabla u(s)) ds \quad \text{for } n \geq 1. \quad (2.5)$$

The classical exponential integrator (for example, the exponential Euler method) approximates  $u(s)$  by  $u(t_{n-1})$  in (2.5). Since

$$u(s) = u(t_{n-1}) + \mu \int_{t_{n-1}}^s A u(\sigma) d\sigma - \int_{t_{n-1}}^s P_X(u(\sigma) \cdot \nabla u(\sigma)) d\sigma, \quad (2.6)$$

substituting this identity into (2.5) yields that

$$u(t_n) = e^{\tau_n \mu A} u(t_{n-1}) - \int_{t_{n-1}}^{t_n} e^{(t_n-s)\mu A} P_X(u(t_{n-1}) \cdot \nabla u(t_{n-1})) ds + R_n, \quad (2.7)$$

where the remainder  $R_n$  is given by

$$\begin{aligned} R_n &= - \int_{t_{n-1}}^{t_n} e^{(t_n-s)\mu A} P_X [u(s) \cdot \nabla u(s) - u(t_{n-1}) \cdot \nabla u(t_{n-1})] ds \\ &= - \int_{t_{n-1}}^{t_n} e^{(t_n-s)\mu A} P_X [(u(s) - u(t_{n-1})) \cdot \nabla u(s)] ds \\ &\quad - \int_{t_{n-1}}^{t_n} e^{(t_n-s)\mu A} P_X [u(t_{n-1}) \cdot \nabla (u(s) - u(t_{n-1}))] ds. \end{aligned}$$

By using the expression of  $u(s) - u(t_{n-1})$  in (2.6), one can obtain the following estimate:

$$\begin{aligned} \|R_n\|_{L^2} &\lesssim \tau_n \|u(s) - u(t_{n-1})\|_{L^\infty(0, T; L^2)} \|\nabla u\|_{L^\infty(0, T; L^\infty)} \\ &\quad + \tau_n \|u\|_{L^\infty(0, T; L^\infty)} \|\nabla (u(s) - u(t_{n-1}))\|_{L^\infty(0, T; L^2)} \\ &\lesssim \mu \tau_n^2 \|u\|_{L^\infty(0, T; H^2)} \|u\|_{L^\infty(0, T; W^{1, \infty})} + \tau_n^2 \|u \cdot \nabla u\|_{L^\infty(0, T; L^2)} \|u\|_{L^\infty(0, T; W^{1, \infty})} \\ &\quad + \mu \tau_n^2 \|u\|_{L^\infty(0, T; L^\infty)} \|u\|_{L^\infty(0, T; H^3)} + \tau_n^2 \|u\|_{L^\infty(0, T; L^\infty)} \|u \cdot \nabla u\|_{L^\infty(0, T; H^1)} \\ &\lesssim \mu \tau_n^2 \|u\|_{L^\infty(0, T; H^2)} \|u\|_{L^\infty(0, T; H^3)} + \tau_n^2 \|u\|_{L^\infty(0, T; H^2)}^2 \|u\|_{L^\infty(0, T; H^3)}. \end{aligned} \quad (2.8)$$

This requires  $u \in L^\infty(0, T; H^3)$  in order to have first-order convergence in time (with second-order local truncation error).

In contrast, the idea behind the low-regularity integrator recently developed in [30] lies in iterating the variation of constants formula (2.5), i.e., approximating  $u(s)$  by  $e^{(s-t_{n-1})\mu A}u(t_{n-1})$  in (2.5) and utilizing the relation

$$u(s) = e^{(s-t_{n-1})\mu A}u(t_{n-1}) - \int_{t_{n-1}}^s e^{(t_n-\sigma)\mu A}P_X(u(\sigma) \cdot \nabla u(\sigma))d\sigma. \quad (2.9)$$

We then rewrite the corresponding temporal integral by

$$\begin{aligned} & \int_{t_{n-1}}^{t_n} e^{(t_n-s)\mu A}P_X(u(s) \cdot \nabla u(s))ds \\ &= \int_{t_{n-1}}^{t_n} e^{(t_n-s)\mu A}P_X(e^{(s-t_{n-1})\mu A}u(t_{n-1}) \cdot \nabla e^{(s-t_{n-1})\mu A}u(t_{n-1}))ds + R_{n,1}. \end{aligned} \quad (2.10)$$

Compared with the formula (2.6) used in the classical exponential integrator, the relation (2.9) does not contain the term  $Au$ . As a result, the remainder  $R_{n,1}$  in (2.10) satisfies the following improved estimate:

$$\|R_{n,1}\|_{L^2} \lesssim \tau_n^2 \|u\|_{L^\infty(0,T;L^\infty)}^2 \|u\|_{L^\infty(0,T;H^2)} + \tau_n^2 \|u\|_{L^\infty(0,T;L^\infty)} \|u\|_{L^\infty(0,T;W^{1,4})}^2, \quad (2.11)$$

which does not contain the  $H^3$  norms of  $u$  that appear in (2.8).

By substituting (2.10) into (2.5), we obtain

$$\begin{aligned} u(t_n) &= e^{\tau_n \mu A} u(t_{n-1}) - \int_{t_{n-1}}^{t_n} e^{(t_n-s)\mu A} P_X(e^{(s-t_{n-1})\mu A} u(t_{n-1}) \cdot \nabla e^{(s-t_{n-1})\mu A} u(t_{n-1})) ds - R_{n,1} \\ &= e^{\tau_n \mu A} u(t_{n-1}) - \int_{t_{n-1}}^{t_n} g(s) ds - R_{n,1}, \end{aligned} \quad (2.12)$$

where

$$g(s) = e^{(t_n-s)\mu A} P_X[v(s) \cdot \nabla v(s)] \quad \text{with} \quad v(s) = e^{(s-t_{n-1})\mu A} u(t_{n-1}).$$

Then we consider a Taylor series of the function  $g(s)$  at  $s = t_n$ . Since (2.3) and (2.4) imply that  $AP_X f = P_X \Delta f = \Delta P_X f$ , by using this relation with  $f = v(s) \cdot \nabla v(s)$  (in the second equality below) we have

$$\begin{aligned} g'(s) &= -e^{(t_n-s)\mu A} \mu A P_X[v(s) \cdot \nabla v(s)] \\ &\quad + e^{(t_n-s)\mu A} P_X[\mu A v(s) \cdot \nabla v(s) + v(s) \cdot \nabla \mu A v(s)] \\ &= -\mu e^{(t_n-s)\mu A} P_X \Delta[v(s) \cdot \nabla v(s)] \\ &\quad + \mu e^{(t_n-s)\mu A} P_X[\Delta v(s) \cdot \nabla v(s) + v(s) \cdot \nabla \Delta v(s)] \\ &= -\mu e^{(t_n-s)\mu A} P_X[v(s) \cdot \nabla \Delta v(s) + \Delta v(s) \cdot \nabla v(s) + \sum_j \partial_j v(s) \cdot \nabla \partial_j v(s)] \\ &\quad + \mu e^{(t_n-s)\mu A} P_X[\Delta v(s) \cdot \nabla v(s) + v(s) \cdot \nabla \Delta v(s)] \\ &= -\mu e^{(t_n-s)\mu A} P_X[\sum_j \partial_j v(s) \cdot \nabla \partial_j v(s)]. \end{aligned} \quad (2.13)$$

Since  $g(s) = g(t_n) - \int_s^{t_n} g'(\sigma) d\sigma$  and

$$\begin{aligned} \|g'(\sigma)\|_{L^2} &\lesssim \mu \|\nabla v(\sigma)\|_{L^q} \|\nabla^2 v(\sigma)\|_{L^p} \quad \text{when} \quad \frac{1}{p} + \frac{1}{q} = \frac{1}{2}, \\ W^{2,p} &\hookrightarrow W^{1,q} \quad \text{when} \quad 1 = \frac{d}{p} - \frac{d}{q} \quad \text{and} \quad 1 \leq p \leq q < \infty, \end{aligned}$$

by choosing  $1 \leq p \leq q < \infty$  satisfying  $\frac{1}{p} + \frac{1}{q} = \frac{1}{2}$  and  $1 = \frac{d}{p} - \frac{d}{q} = \frac{2d}{p} - \frac{d}{2}$  we obtain

$$\|g'(\sigma)\|_{L^2} \lesssim \mu \|v(\sigma)\|_{W^{2,p}}^2 \quad (2.14)$$

with

$$p = \begin{cases} \frac{2d}{1+d/2} = \frac{12}{5} & \text{if } d = 3 \\ 2 + \epsilon & \text{if } d = 2, \end{cases} \quad (2.15)$$

where  $\epsilon > 0$  can be arbitrarily small. Therefore, the following result holds:

$$\|g(s) - g(t_n)\|_{L^2} \lesssim \mu \tau_n \|v\|_{L^\infty(0,T;W^{2,p})}^2 \lesssim \mu \tau_n \|u\|_{L^\infty(0,T;W^{2,p})}^2.$$

In view of this estimate, we can rewrite (2.12) as

$$u(t_n) = e^{\tau_n \mu A} u(t_{n-1}) - \int_{t_{n-1}}^{t_n} g(t_n) ds - R_{n,1} - R_{n,2}, \quad (2.16)$$

with a new remainder  $R_{n,2}$  which has the following bound:

$$\|R_{n,2}\|_{L^2} \lesssim \mu \tau_n^2 \|u\|_{L^\infty(0,T;W^{2,p})}^2. \quad (2.17)$$

Inserting the expression of  $g(t_n)$  into (2.16), we have

$$u(t_n) = e^{\tau_n \mu A} u(t_{n-1}) - \tau_n P_X [e^{\tau_n \mu A} u(t_{n-1}) \cdot \nabla e^{\tau_n \mu A} u(t_{n-1})] - R_{n,1} - R_{n,2}. \quad (2.18)$$

Dropping the remainders  $R_{n,1}$  and  $R_{n,2}$  in (2.18) would yield a fully explicit scheme

$$u_n = e^{\tau_n \mu A} u_{n-1} - \tau_n P_X [e^{\tau_n \mu A} u_{n-1} \cdot \nabla e^{\tau_n \mu A} u_{n-1}]. \quad (2.19)$$

However, in the stability estimate the gradient on the right-hand side should be bounded by the smoothing property of the semigroup  $e^{\tau_n \mu A}$ , and this would yield a stability estimate which depend on  $\mu^{-1}$ . This would not be suitable for solving the NS equations when the viscosity  $\mu$  is small.

In order to construct a low-regularity integrator which is stable for small  $\mu$ , we further approximate  $\nabla e^{\tau_n \mu A} u(t_{n-1})$  by  $\nabla u(t_n)$ , and rewrite (2.18) into

$$u(t_n) = e^{\tau_n \mu A} u(t_{n-1}) - \tau_n P_X [e^{\tau_n \mu A} u(t_{n-1}) \cdot \nabla u(t_n)] - R_{n,1} - R_{n,2} - P_X R_{n,3}, \quad (2.20)$$

with

$$\begin{aligned} R_{n,3} &= \tau_n e^{\tau_n \mu A} u(t_{n-1}) \cdot \nabla [e^{\tau_n \mu A} u(t_{n-1}) - u(t_n)] \\ &= \tau_n e^{\tau_n \mu A} u(t_{n-1}) \cdot \nabla \int_{t_{n-1}}^{t_n} e^{(t_n-s)\mu A} P_X (u(s) \cdot \nabla u(s)) ds \quad (\text{here (2.5) is used}) \\ &= \tau_n [e^{\tau_n \mu A} u(t_{n-1})]_j \cdot \int_{t_{n-1}}^{t_n} e^{(t_n-s)\mu A} P_X (u(s) \cdot \nabla \partial_j u(s)) ds \\ &\quad + \tau_n [e^{\tau_n \mu A} u(t_{n-1})]_j \cdot \int_{t_{n-1}}^{t_n} e^{(t_n-s)\mu A} P_X (\partial_j u(s) \cdot \nabla u(s)) ds, \end{aligned} \quad (2.21)$$

where we have used (2.5) in deriving the second to last inequality. The new remainder has the following bound:

$$\begin{aligned} \|R_{n,3}\|_{L^2} &\lesssim \tau_n^2 \|e^{\tau_n \mu A} u(t_{n-1})\|_{L^\infty} \|u\|_{L^\infty(0,T;L^\infty)} \|u\|_{L^\infty(0,T;H^2)} \\ &\quad + \tau_n^2 \|e^{\tau_n \mu A} u(t_{n-1})\|_{L^\infty} \|u\|_{L^\infty(0,T;W^{1,4})}^2 \\ &\lesssim \tau_n^2 \|u\|_{L^\infty(0,T;H^2)}^3. \end{aligned} \quad (2.22)$$

Hence, the remainders in (2.20) are bounded by  $O(\tau_n^2)$  in the  $L^2$  norm, i.e.,

$$\|R_{n,1}\|_{L^2} + \|R_{n,2}\|_{L^2} + \|R_{n,3}\|_{L^2} \lesssim \tau_n^2, \quad (2.23)$$

which only requires  $u \in L^\infty(0, T; W^{2,p})$ , where  $p$  is defined in (2.15).

By dropping the remainders  $R_{n,1}$ ,  $R_{n,2}$  and  $P_X R_{n,3}$  in (2.20), we obtain the following semi-implicit exponential method for the NS equations:

$$u_n + \tau_n P_X [e^{\tau_n \mu A} u_{n-1} \cdot \nabla u_n] = e^{\tau_n \mu A} u_{n-1}. \quad (2.24)$$

## 2.2. Extension to the no-slip boundary condition

If  $\Omega$  is a bounded domain in  $\mathbb{R}^d$  and the NS equations are considered under the no-slip boundary condition, i.e.,  $u = 0$  on  $\partial\Omega$ , then the definition of  $\dot{H}$  should be replaced by

$$\dot{H} = \{v \in L^2(\Omega)^d : \nabla \cdot v = 0, \quad v \cdot \nu = 0 \text{ on } \partial\Omega\},$$

where  $\nu$  denotes the unit outward normal vector on the boundary  $\partial\Omega$ . The  $L^2$ -orthogonal projection  $P_X : L^2(\Omega)^d \rightarrow \dot{H}$  is given by

$$P_X f = f - \nabla q, \quad (2.25)$$

where  $q$  is the solution (up to a constant) of the following elliptic boundary value problem:

$$\begin{cases} \Delta q = \nabla \cdot f \\ \nabla q \cdot \nu = f \cdot \nu. \end{cases}$$

Let  $\dot{H}^2 = \{v \in (H_0^1 \times H^2)^d : \nabla \cdot v = 0\}$  and  $A = P_X \Delta : \dot{H}^2 \rightarrow \dot{H}$ . Then the NS equations can be written as (2.2). Since  $P_X \nabla q = 0$  for  $q \in H^1(\Omega)^d$ , applying  $A = P_X \Delta$  to (2.25) yields

$$A P_X f = P_X \Delta f \quad \text{for } f \in (H_0^1 \times H^2)^d, \quad (2.26)$$

which is the same as (2.3). But (2.4) should be replaced by

$$A v = P_X \Delta v = \Delta v - \nabla r \quad \text{for } v \in \dot{H}^2, \quad (2.27)$$

where

$$\begin{cases} \Delta r = \nabla \cdot \Delta v \\ \nabla r \cdot \nu = \Delta v \cdot \nu. \end{cases} \quad (2.28)$$

In a bounded Lipschitz domain it is known that the solution of (2.28) satisfies the basic  $W^{1,p}$  estimate for some sufficiently small number  $\epsilon_* > 0$  (see [16, Theorem 2]):

$$\|r\|_{W^{1,p}} \lesssim \|v\|_{W^{2,p}} \quad \text{for } 2 \leq p < 3 + \epsilon_*. \quad (2.29)$$

The change from (2.4) to (2.27) causes the change of analysis in the local truncation errors in (2.13), i.e.,

$$\begin{aligned} g'(s) &= -e^{(t_n-s)\mu A} \mu A P_X [v(s) \cdot \nabla v(s)] \\ &\quad + e^{(t_n-s)\mu A} P_X [\mu A v(s) \cdot \nabla v(s) + v(s) \cdot \nabla \mu A v(s)] \\ &= -\mu e^{(t_n-s)\mu A} P_X \Delta [v(s) \cdot \nabla v(s)] \\ &\quad + \mu e^{(t_n-s)\mu A} P_X [(\Delta v(s) - \nabla r) \cdot \nabla v(s) + v(s) \cdot \nabla (\Delta v(s) - \nabla r)] \\ &= -\mu e^{(t_n-s)\mu A} P_X [v(s) \cdot \nabla \Delta v(s) + \Delta v(s) \cdot \nabla v(s) + \sum_j \partial_j v(s) \cdot \nabla \partial_j v(s)] \end{aligned}$$

$$\begin{aligned}
& + \mu e^{(t_n-s)\mu A} P_X [\Delta v(s) \cdot \nabla v(s) + v(s) \cdot \nabla \Delta v(s)] \\
& - \mu e^{(t_n-s)\mu A} P_X [\partial_j r \partial_j v(s) + v_j(s) \partial_j \nabla r] \\
= & - \mu e^{(t_n-s)\mu A} P_X [\sum_j \partial_j v(s) \cdot \nabla \partial_j v(s)] \\
& - \mu e^{(t_n-s)\mu A} P_X [\partial_j r \partial_j v(s) + v_j(s) \partial_j \nabla r], \tag{2.30}
\end{aligned}$$

where some additional terms involving  $\nabla^2 r$  appears, compared with (2.13). Since  $\|\nabla^2 r\|_{L^2}$  is equivalent to  $\|v\|_{H^3}$ , the additional term involving  $\nabla^2 r$  is not desired. Fortunately, the projection operator  $P_X$  in the last term of (2.30) cancels this bad term, i.e.,

$$\begin{aligned}
(2.30) = & - \mu e^{(t_n-s)\mu A} P_X [\sum_j \partial_j v(s) \cdot \nabla \partial_j v(s)] \\
& - \mu e^{(t_n-s)\mu A} P_X [\partial_j r \cdot \partial_j v(s) - \nabla v_j(s) \partial_j r] \\
& - \mu e^{(t_n-s)\mu A} P_X [\nabla(v_j(s) \cdot \partial_j r)]. \tag{2.31}
\end{aligned}$$

Since  $P_X \nabla q = 0$  for all  $q \in H^1(\Omega)$ , it follows that the last term of (2.31) is zero. This implies that

$$\begin{aligned}
g'(s) = & - \mu e^{(t_n-s)\mu A} P_X [\sum_j \partial_j v(s) \cdot \nabla \partial_j v(s)] \\
& - \mu e^{(t_n-s)\mu A} P_X [\partial_j r \cdot \partial_j v(s) - \nabla v_j(s) \partial_j r]. \tag{2.32}
\end{aligned}$$

If  $2 \leq p \leq q < \infty$ ,  $\frac{1}{p} + \frac{1}{q} = \frac{1}{2}$  and  $p < 3 + \epsilon_*$ , then

$$\begin{aligned}
\|g'(s)\|_{L^2} & \lesssim \mu \|\nabla v(s)\|_{L^q} (\|\nabla^2 v(s)\|_{L^p} + \|\nabla r\|_{L^p}) \\
& \lesssim \mu \|\nabla v(s)\|_{L^q} \|\nabla^2 v(s)\|_{L^p} \quad (\text{here (2.29) is used}).
\end{aligned}$$

Since

$$W^{2,p} \hookrightarrow W^{1,q} \quad \text{when } 1 = \frac{d}{p} - \frac{d}{q} \text{ and } 1 \leq p \leq q < \infty,$$

by choosing  $2 \leq p \leq q < \infty$  satisfying  $\frac{1}{p} + \frac{1}{q} = \frac{1}{2}$  and  $1 = \frac{d}{p} - \frac{d}{q} = \frac{2d}{p} - \frac{d}{2}$  we obtain

$$\|g'(s)\|_{L^2} \lesssim \mu \|v(s)\|_{W^{2,p}}^2 \tag{2.33}$$

with

$$p = \begin{cases} \frac{12}{5} & \text{if } d = 3 \\ 2 + \epsilon & \text{if } d = 2, \end{cases}$$

where  $\epsilon > 0$  can be arbitrarily small. Indeed, this choice of  $p$  satisfies the condition  $p < 3 + \epsilon_*$  required in (2.29). Since the estimate (2.33) we obtained here is the same as (2.14), the rest analysis would be the same as the periodic boundary condition and therefore omitted. In the end, we would obtain (2.20) under the no-slip boundary condition, with remainders  $R_{n,1}$ ,  $R_{n,2}$  and  $R_{n,3}$  satisfying the same estimates as that under periodic boundary conditions. By dropping the remainders we would obtain the same semi-implicit exponential method (2.24).

### 2.3. The energy-decay property

The proposed semi-implicit exponential low-regularity integrator in (2.24) preserves the energy-decay structure of the NS equations. This can be seen by testing (2.24) with  $u_n$ . Then we have

$$\|u_n\|_{L^2}^2 + \tau_n (e^{\tau_n \mu A} u_{n-1} \cdot \nabla u_n, u_n) = (e^{\tau_n \mu A} u_{n-1}, u_n). \tag{2.34}$$

Since  $e^{\tau_n \mu A} u_{n-1}$  is divergence-free (the same as  $u_{n-1}$ ), it follows from integration by parts that

$$(e^{\tau_n \mu A} u_{n-1} \cdot \nabla u_n, u_n) = (e^{\tau_n \mu A} u_{n-1}, \nabla \frac{1}{2} |u_n|^2) = -(\nabla \cdot (e^{\tau_n \mu A} u_{n-1}), \frac{1}{2} |u_n|^2) = 0.$$

As a result, (2.34) reduces to

$$\|u_n\|_{L^2}^2 = (e^{\tau_n \mu A} u_{n-1}, u_n) \leq \|e^{\tau_n \mu A} u_{n-1}\|_{L^2} \|u_n\|_{L^2} \leq \|u_{n-1}\|_{L^2} \|u_n\|_{L^2},$$

which implies that

$$\|u_n\|_{L^2} \leq \|u_{n-1}\|_{L^2}. \quad (2.35)$$

On the one hand, the energy-decay structure of the semi-implicit exponential low-regularity integrator guarantees the energy boundedness of the numerical solution without requiring any regularity of the solution and initial data. On the other hand, this energy-decay structure also plays an important role in guaranteeing the convergence of numerical solutions when the solution has sufficient regularity, as reflected by the error analysis below.

#### 2.4. Error estimates

**Theorem 2.1.** *Consider the NS equations either in a torus  $\Omega = [0, 1]^d$  with periodic boundary condition or in a bounded domain  $\Omega$  under the Dirichlet boundary condition, and assume that the solution of the NS equations has the following regularity:*

$$u \in C([0, T]; L^2(\Omega)^d) \cap L^\infty(0, T; W^{1,\infty}(\Omega)^d) \cap L^\infty(0, T; W^{2,p}(\Omega)^d), \quad (2.36)$$

where  $p$  is given by (2.15). Then the numerical solution by the semi-implicit exponential method (2.24) has the following error bound:

$$\max_{1 \leq n \leq N} \|e_n\|_{L^2} \lesssim \tau. \quad (2.37)$$

*Proof.* If the solution has regularity (2.36) for some  $p > d$ , then  $p$  is bigger than the value defined in (2.15) and therefore the regularity required in Section 2 is satisfied.

Let  $e_n = u_n - u(t_n)$  be the error function. The difference between (2.24) and (2.20) yields the following error equation:

$$\begin{aligned} e_n + \tau_n P_X [e^{\tau_n \mu A} u_{n-1} \cdot \nabla e_n] &= e^{\tau_n \mu A} e_{n-1} - \tau_n P_X [e^{\tau_n \mu A} e_{n-1} \cdot \nabla u(t_n)] \\ &\quad + R_{n,1} + R_{n,2} + P_X R_{n,3}. \end{aligned} \quad (2.38)$$

Testing (2.38) by  $e_n$  and using the consistency error estimates in (2.23), we obtain

$$\begin{aligned} \|e_n\|_{L^2}^2 &= (e^{\tau_n \mu A} e_{n-1}, e_n) - (\tau_n e^{\tau_n \mu A} e_{n-1} \cdot \nabla u(t_n), e_n) + (R_{n,1} + R_{n,2} + P_X R_{n,3}, e_n) \\ &\leq \frac{1}{2} \|e_{n-1}\|_{L^2}^2 + \frac{1}{2} \|e_n\|_{L^2}^2 + C\tau_n \|\nabla u(t_n)\|_{L^\infty} \|e_{n-1}\|_{L^2} \|e_n\|_{L^2} + C\tau_n^2 \|e_n\|_{L^2}^2 \\ &\leq \frac{1}{2} \|e_{n-1}\|_{L^2}^2 + \frac{1}{2} \|e_n\|_{L^2}^2 + C\tau_n \|e_{n-1}\|_{L^2}^2 + C\tau_n \|e_n\|_{L^2}^2 + C\tau_n^3. \end{aligned}$$

The second and fourth terms on the right-hand side can be absorbed by the left-hand side. Therefore, we have

$$(1 - C\tau_n) \|e_n\|_{L^2}^2 \leq (1 + C\tau_n) \|e_{n-1}\|_{L^2}^2 + C\tau_n^3.$$

For sufficiently small stepsize  $\tau_n$  we can apply Gronwall's inequality. This yields

$$\max_{1 \leq n \leq N} \|e_n\|_{L^2}^2 \lesssim \tau^2.$$

This proves the desired error bound in Theorem 2.1.  $\square$

### 3. Extension to full discretization

In this section, we show that the proposed semi-implicit exponential method in (2.24) can be extended to full discretization, for example, with finite element methods or spectral methods in space. Since the error analysis of these two class of full discretizations are similar, we present the error analysis only for the finite element method in this article.

#### 3.1. A finite element method with postprocessing

In this subsection, we extend the low-regularity integrator to full discretization by using a finite element method with postprocessing at every time level. For simplicity we focus on the periodic boundary condition.

We consider a conforming finite element subspace  $X_h \times M_h \subset H^1(\Omega)^d \times L^2(\Omega)$  with the following two properties:

(1) The inf-sup condition:

$$\|q^h\|_{L^2} \lesssim \sup_{\substack{v^h \in X_h \\ v^h \neq 0}} \frac{(\nabla \cdot v^h, q^h)}{\|v^h\|_{H^1}}.$$

(2) Approximation properties:

$$\begin{aligned} \inf_{v^h \in X_h} (\|v - v^h\|_{L^2} + h\|v - v^h\|_{H^1}) &\lesssim h^k \|v\|_{H^k} && \text{for } v \in H^k(\Omega)^d \text{ and } 1 \leq k \leq 2, \\ \inf_{q^h \in M_h} \|q - q^h\|_{L^2} &\lesssim h^k \|q\|_{H^k} && \text{for } q \in H^k(\Omega) \text{ and } 0 \leq k \leq 1. \end{aligned}$$

Examples of such finite element spaces include the Taylor–Hood  $P^k$ - $P^{k-1}$  spaces (for  $k \geq 2$ ) and the mini-element  $P^{1b}$ - $P^1$  space; see [2, 4, 5].

We define the discrete divergence-free subspace of  $X_h$  by

$$\dot{X}_h = \{v^h \in X_h : (\nabla \cdot v^h, q^h) = 0 \text{ for all } q^h \in M_h\},$$

and then define the discrete Stokes operator  $A_h : \dot{X}_h \rightarrow \dot{X}_h$  by

$$(A_h w^h, v^h) = -(\nabla w^h, \nabla v^h) \quad \forall w^h, v^h \in \dot{X}_h.$$

We define  $U_h$  to be the  $H(\text{div}, \Omega)$ -conforming Raviart–Thomas finite element spaces of order 1, i.e.,

$$U_h := \{w \in H(\text{div}, \Omega) : w|_K \in P_1(K)^d + xP_1(K) \text{ for every triangle } K\},$$

and define the divergence-free subspace of  $U_h$  by

$$\dot{U}_h := \{v_h \in U_h : \nabla \cdot v_h = 0 \text{ in } \Omega\}. \quad (3.1)$$

Let  $P_{\dot{U}_h} : L^2(\Omega)^d \rightarrow \dot{U}_h$  be the  $L^2$ -orthogonal projection, defined by

$$(v - P_{\dot{U}_h} v, w_h) = 0 \quad \forall w_h \in \dot{U}_h, \quad \forall v \in L^2(\Omega)^d. \quad (3.2)$$

If  $v \in H^2(\Omega)^d$  is a divergence-free vector field then the following approximation result holds (see [21, inequality (3.4)])

$$\|v - P_{\dot{U}_h} v\|_{L^2} \leq Ch^2 \|v\|_{H^2}. \quad (3.3)$$

Note that the weak formulation of the time-stepping method in (2.24) can be written as

$$(u_n, v) + (\tau_n e^{\tau_n \mu A} u_{n-1} \cdot \nabla u_n, v) + (p_n, \nabla \cdot v) = (e^{\tau_n \mu A} u_{n-1}, v) \quad \forall v \in H^1(\Omega)^d, \quad (3.4)$$

$$(\nabla \cdot u_n, q) = 0 \quad \forall q \in L^2(\Omega), \quad (3.5)$$

where  $p_n$  is the function satisfying

$$\tau_n P_X [e^{\tau_n \mu A} u_{n-1} \cdot \nabla u_n] = \tau_n e^{\tau_n \mu A} u_{n-1} \cdot \nabla u_n - \nabla p_n.$$

By using the discrete Stokes operator  $A_h$  and the projection operator  $P_{\dot{U}_h}$  introduced in this section, we consider the following fully discrete finite element method for (3.4)–(3.5): Find  $(u_n^h, p_n^h) \in X_h \times M_h$  such that the following equations hold:

$$(u_n^h, v^h) + \tau_n ([P_{\dot{U}_h} e^{\tau_n \mu A_h} u_{n-1}^h] \cdot \nabla u_n^h, v^h) + (p_n^h, \nabla \cdot v^h) = (e^{\tau_n \mu A_h} u_{n-1}^h, v^h) \quad \forall v^h \in X_h, \quad (3.6)$$

$$(\nabla \cdot u_n^h, q^h) = 0 \quad \forall q^h \in M_h. \quad (3.7)$$

The presence of the postprocessing projection  $P_{\dot{U}_h}$  is necessary for obtaining error estimates as well as preserving the energy-decay structure. In particular, since  $\tau_n P_{\dot{U}_h} e^{\tau_n \mu A_h} u_{n-1}^h$  is divergence-free (due to the projection  $P_{\dot{U}_h}$ ), it follows that

$$\tau_n ([P_{\dot{U}_h} e^{\tau_n \mu A_h} u_{n-1}^h] \cdot \nabla u_n^h, u_n^h) = 0.$$

As a result, choosing  $(v^h, q^h) = (u_n^h, p_n^h)$  in (3.6)–(3.7) yields

$$\|u_n^h\|_{L^2}^2 = (e^{\tau_n \mu A_h} u_{n-1}^h, u_n^h) \leq \|e^{\tau_n \mu A_h} u_{n-1}^h\|_{L^2} \|u_n^h\|_{L^2} \leq \|u_{n-1}^h\|_{L^2} \|u_n^h\|_{L^2}, \quad (3.8)$$

which implies the following energy-decay inequality:

$$\|u_n^h\|_{L^2} \leq \|u_{n-1}^h\|_{L^2}. \quad (3.9)$$

**Theorem 3.1.** *Consider the NS equations either in a torus  $\Omega = [0, 1]^d$  (with periodic boundary condition) and assume that the solution of the NS problem (1.1) has the following regularity:*

$$u \in C([0, T]; L^2(\Omega)^d) \cap L^\infty(0, T; W^{1,\infty}(\Omega)^d) \cap L^\infty(0, T; W^{2,p}(\Omega)^d), \quad (3.10)$$

where  $p$  is given by (2.15). Then, under mesh size restriction  $h \lesssim \tau_{\min}$  (the smallest stepsize), the numerical solution given by the fully discrete method (3.6)–(3.7) has the following error bound:

$$\max_{1 \leq n \leq N} \|u_n^h - u(t_n)\|_{L^2} \lesssim \tau. \quad (3.11)$$

*Proof.* By requiring the test function  $v^h$  to be in the discrete divergence-free subspace  $\dot{X}_h$ , the weak formulation (3.6)–(3.7) can be equivalently written as: Find  $u_n^h \in \dot{X}_h$  such that

$$(u_n^h, v^h) + \tau_n (P_{\dot{U}_h} [e^{\tau_n \mu A_h} u_{n-1}^h] \cdot \nabla u_n^h, v^h) = (e^{\tau_n \mu A_h} u_{n-1}^h, v^h) \quad \forall v^h \in \dot{X}_h. \quad (3.12)$$

The exact solution satisfies similar equations, i.e.,

$$(P_{\dot{X}_h} u(t_n), v^h) + \tau_n (P_{\dot{U}_h} [e^{\tau_n \mu A_h} P_{\dot{X}_h} u(t_{n-1})] \cdot \nabla P_{\dot{X}_h} u(t_n), v^h)$$

$$\begin{aligned}
&= (e^{\tau_n \mu A_h} P_{\dot{X}_h} u(t_{n-1}), v^h) - (R_{n,1} + R_{n,2} + P_X R_{n,3}, v^h) \\
&\quad - (E_{n,1} + E_{n,2} + E_{n,3}, v^h) \quad \forall v^h \in \dot{X}_h, \quad (3.13)
\end{aligned}$$

where

$$E_{n,1} = \tau_n [e^{\tau_n \mu A} u(t_{n-1}) - P_{\dot{U}_h} e^{\tau_n \mu A_h} P_{\dot{X}_h} u(t_{n-1})] \cdot \nabla u(t_n), \quad (3.14)$$

$$E_{n,2} = \tau_n P_{\dot{U}_h} [e^{\tau_n \mu A_h} P_{\dot{X}_h} u(t_{n-1})] \cdot \nabla (u(t_n) - P_{\dot{X}_h} u(t_n)), \quad (3.15)$$

$$E_{n,3} = e^{\tau_n \mu A_h} P_{\dot{X}_h} u(t_{n-1}) - P_{\dot{X}_h} e^{\tau_n \mu A} u(t_{n-1}). \quad (3.16)$$

By using the triangle inequality we can decompose  $E_{n,1}$  into two parts, i.e.,

$$\|E_{n,1}\|_{L^2} \leq \tau_n \left\| [e^{\tau_n \mu A} u(t_{n-1}) - P_{\dot{U}_h} e^{\tau_n \mu A} u(t_{n-1})] \cdot \nabla u(t_n) \right\|_{L^2} \quad (3.17)$$

$$\begin{aligned}
&+ \tau_n \left\| P_{\dot{U}_h} [e^{\tau_n \mu A} u(t_{n-1}) - e^{\tau_n \mu A_h} P_{\dot{X}_h} u(t_{n-1})] \cdot \nabla u(t_n) \right\|_{L^2} \\
&\leq \tau_n h^2 \|e^{\tau_n \mu A} u(t_{n-1})\|_{H^2} \|\nabla u(t_n)\|_{L^\infty} + \tau_n h^2 \|u(t_{n-1})\|_{H^2} \|\nabla u(t_n)\|_{L^\infty}, \quad (3.18)
\end{aligned}$$

where the first term on the right-hand side of (3.17) is estimated by using (3.3), and the second term is estimated by using the standard  $L^2$  error estimates of semidiscrete FEM for a linear parabolic equation with initial value  $u(t_{n-1})$ ; see [35, Theorem 3.1] (for the time-dependent Stokes equations the error estimation is the same). The standard approximation property of the  $L^2$  projection operator  $P_{\dot{X}_h}$  implies that

$$\|E_{n,2}\|_{L^2} \lesssim \tau_n h \|u\|_{L^\infty(0,T;H^2)}. \quad (3.19)$$

Again, the standard  $L^2$  error estimates of semidiscrete FEM for linear parabolic equations with initial value  $u(t_{n-1})$  in [35, Theorem 3.1] implies that

$$\|E_{n,3}\|_{L^2} \lesssim h^2 \|u(t_{n-1})\|_{H^2}. \quad (3.20)$$

The three estimates above can be summarized as

$$\|E_{n,1}\|_{L^2} + \|E_{n,2}\|_{L^2} + \|E_{n,3}\|_{L^2} \lesssim \tau_n h + h^2. \quad (3.21)$$

Let  $e_n^h = u_n^h - P_{\dot{X}_h} u(t_n)$ . Then the difference between (3.12) and (3.13) yields the following error equation:

$$\begin{aligned}
&(e_n^h, v^h) + \tau_n (P_{\dot{U}_h} [e^{\tau_n \mu A_h} u_{n-1}^h] \cdot \nabla e_n^h, v^h) + \tau_n (P_{\dot{U}_h} [e^{\tau_n \mu A_h} e_{n-1}^h] \cdot \nabla P_{\dot{X}_h} u(t_n), v^h) \\
&= (e^{\tau_n \mu A_h} e_{n-1}^h, v^h) - (R_{n,1} + R_{n,2} + P_X R_{n,3}, v^h) - (E_{n,1} + E_{n,2} + E_{n,3}, v^h) \quad \forall v^h \in \dot{X}_h.
\end{aligned} \quad (3.22)$$

By choosing  $v^h = e_n^h$  in (3.22) and using the property (thanks to the projection  $P_{\dot{U}_h}$  onto the divergence-free space  $\dot{U}_h$ )

$$(P_{\dot{U}_h} [e^{\tau_n \mu A_h} u_{n-1}^h] \cdot \nabla e_n^h, e_n^h) = 0,$$

we obtain

$$\begin{aligned}
&\|e_n^h\|_{L^2}^2 + \tau_n (P_{\dot{U}_h} [e^{\tau_n \mu A_h} e_{n-1}^h] \cdot \nabla P_{\dot{X}_h} u(t_n), e_n^h) \\
&= (e^{\tau_n \mu A_h} e_{n-1}^h, e_n^h) - (R_{n,1} + R_{n,2} + P_X R_{n,3}, e_n^h) - (E_{n,1} + E_{n,2} + E_{n,3}, e_n^h). \quad (3.23)
\end{aligned}$$

The right-hand side of the above inequality can be estimated by using the consistency error estimates in (2.23) and (3.21). This yields

$$\|e_n^h\|_{L^2}^2 + \tau_n (P_{\dot{U}_h} [e^{\tau_n \mu A_h} e_{n-1}^h] \cdot \nabla P_{\dot{X}_h} u(t_n), e_n^h)$$

$$\begin{aligned}
&\leq \frac{1}{2}\|e_{n-1}^h\|_{L^2}^2 + \frac{1}{2}\|e_n^h\|_{L^2}^2 + C\tau_n(\tau_n + h)\|e_n^h\|_{L^2} + Ch^2\|e_n^h\|_{L^2} \\
&\leq \frac{1}{2}\|e_{n-1}^h\|_{L^2}^2 + \frac{1+\tau_n}{2}\|e_n^h\|_{L^2}^2 + C[\tau_n(\tau_n^2 + h^2) + h^4/\tau_n] \\
&\leq \frac{1}{2}\|e_{n-1}^h\|_{L^2}^2 + \frac{1+\tau_n}{2}\|e_n^h\|_{L^2}^2 + C\tau_n^3 \quad \text{when } h \lesssim \tau_n.
\end{aligned} \tag{3.24}$$

The second term on the left-hand side of the above inequality can be estimated by

$$|\tau_n(P_{U_h}[e^{\tau_n\mu A_h}e_{n-1}^h] \cdot \nabla P_{X_h}u(t_n), e_n^h)| \lesssim \tau_n\|e_{n-1}^h\|_{L^2}\|e_n^h\|_{L^2}. \tag{3.25}$$

By combining the two inequalities above, we obtain

$$(1 - \tau_n)\|e_n^h\|_{L^2}^2 \leq (1 + C\tau_n)\|e_{n-1}^h\|_{L^2}^2 + C\tau_n^3 \quad \text{when } h \lesssim \tau_n. \tag{3.26}$$

Then, iterating the inequality for  $n = 1, 2, \dots, N$ , we obtain the following error bound:

$$\max_{1 \leq n \leq N} \|e_n^h\|_{L^2}^2 \lesssim \tau^2 \quad \text{when } h \lesssim \tau_{\min}. \tag{3.27}$$

This completes the proof of Theorem 3.1.  $\square$

### 3.2. A spectral collocation method

In this subsection, we show that the proposed semi-implicit low-regularity exponential integrator can also be combined with some spectral methods which can be performed with less computational cost by using the Fast Fourier transform (FFT). For illustration, we present a Fourier collocation method in the two-dimensional torus. The three dimensional case can be treated similarly by using the eigenfunctions expansion of the Stokes operator; see [37, Theorem 2.11] or [31, Section 7].

It is known that the eigenfunctions of the Stokes operator  $A = P_X\Delta$  on the torus  $\Omega = [-\pi, \pi] \times [-\pi, \pi]$  are the constant vector fields

$$\phi_{01} = \begin{pmatrix} 1 \\ 0 \end{pmatrix} \quad \text{and} \quad \phi_{02} = \begin{pmatrix} 0 \\ 1 \end{pmatrix}$$

and the following vector fields:

$$\phi_k = k^\perp e^{ik \cdot x}, \quad k \in \mathbb{Z}_0^2 := \mathbb{Z}^2 \setminus \{(0, 0)\}, \quad \text{where } k^\perp := \begin{pmatrix} k_2 \\ -k_1 \end{pmatrix},$$

with eigenvalues  $-k^2$  for  $k \in \mathbb{Z}_0^2$ . Let  $X_M = \text{span}\{\phi_{01}, \phi_{02}\} \oplus \text{span}\{\phi_k : |k| \leq M\}$ . If the numerical solution at time level  $t = t_{n-1}$  is known to be

$$u_{n-1}^M = u_{n-1,1}\phi_{01} + u_{n-1,2}\phi_{02} + \sum_{|k| \leq M} u_{n-1,k}\phi_k \in X_M,$$

then we seek a numerical solution at  $t = t_n$ , i.e.,

$$u_n^M = u_{n,1}\phi_{01} + u_{n,2}\phi_{02} + \sum_{|k| \leq M} u_{n,k}\phi_k \in X_M,$$

satisfying the following equation:

$$u_n^M + \tau_n P_{X_M}[e^{\tau_n\mu A}u_{n-1}^M \cdot \nabla u_n^M] = e^{\tau_n\mu A}u_{n-1}^M. \tag{3.28}$$

where  $P_{X_M} : L^2 \rightarrow X_M$  is the  $L^2$ -orthogonal projection.

The Fourier spectral method in (3.28) can be computed by the FFT. In fact, direct calculation yields

$$e^{\tau_n \mu A} u_{n-1}^M = u_{n-1,1} \phi_{01} + u_{n-1,2} \phi_{02} + \sum_{|k| \leq M} e^{-\tau_n \mu k^2} u_{n-1,k} k^\perp e^{ik \cdot x}$$

$$\nabla u_n^M = \sum_{|j| \leq M} i u_{n,j} j \otimes j^\perp e^{ij \cdot x}$$

and therefore

$$\begin{aligned} e^{\tau_n \mu A} u_{n-1}^M \cdot \nabla u_n^M &= \sum_{|m| \leq M} (u_{n-1,1} \phi_{01} + u_{n-1,2} \phi_{02}) i u_{n,m} m \otimes m^\perp e^{im \cdot x} \\ &\quad + \sum_{|m| \leq 2M} \sum_{k+j=m} i e^{-\tau_n \mu k^2} u_{n-1,k} (k^\perp \cdot j) u_{n,j} j^\perp e^{im \cdot x} \\ &=: \sum_{|m| \leq 2M} v_m e^{im \cdot x}. \end{aligned}$$

This is a product of two  $2M$ -term Fourier series, and therefore the coefficients  $v_m$ ,  $|m| \leq 2M$ , can be computed by FFT with computational cost of  $O(M \ln M)$ ; see Appendix. Its projection onto  $X_M$  is given by

$$P_{X_M} [e^{\tau_n \mu A} u_{n-1}^M \cdot \nabla u_n^M] = \sum_{|m| \leq M} v_m \cdot \frac{m^\perp \otimes m^\perp}{(2\pi)^d |m|^2} e^{im \cdot x},$$

which is equivalent to cutting the length of a vector and then multiplying the vector by a diagonal matrix, and therefore can be computed with  $O(M)$  operations.

Overall, the matrix-vector product on the left-hand side of (3.28) can be computed by FFT with computational cost of  $O(M \ln M)$ . Under the condition  $\tau_n = O(h)$ , the condition number of the coefficient matrix in (3.28) is  $O(1)$ . In this case, we can solve the linear system of (3.28) by using GMRES, which converges well when the condition number of the matrix is  $O(1)$ . The errors of the numerical solutions given by this method (versus CPU time) is shown in the numerical experiments in the next section.

#### 4. Numerical experiments

In this section, we present numerical tests to support the theoretical analysis and to illustrate the advantages of the proposed method in comparison with the semi-implicit Euler method and classical exponential integrator (i.e., the exponential Euler method).

We solve the NS equations in the two-dimensional torus  $[0, 1] \times [0, 1]$  under the periodic boundary condition by the proposed exponential low-regularity integrator (Exponential LRI), with initial value

$$u^0 = (u_1^0(x, y), u_2^0(x, y)),$$

where

$$\begin{aligned} u_1^0(x, y) &= m\pi \sin^m(\pi x) \sin^{m-1}(\pi y) \cos(\pi y), \\ u_2^0(x, y) &= -m\pi \sin^{m-1}(\pi x) \sin^m(\pi y) \cos(\pi x). \end{aligned}$$

By choosing  $m = 2.6$ , the initial value satisfies  $u^0 \in H^{2+\epsilon}(\Omega)^2$  for  $0 < \epsilon < 0.1$ . Therefore, the initial value satisfies the conditions in Theorem 3.1. The algorithm in [24] is used to evaluate the exponential operators in the low-regularity integrator and exponential Euler method.

We present the time discretization errors  $\|u_N^{(\tau)} - u_N^{(\tau/2)}\|_{L^2(\Omega)}$  of the numerical solutions at time  $T = 1/8$  in Figure 1 for  $\mu = 0.5, 10^{-2}$  and  $10^{-4}$ . The NaN in the case  $\mu = 10^{-4}$  indicates that the numerical solution of the exponential Euler method blows up due to instability. From the numerical results in Figure 1 we see that the proposed Exponential LRI has first-order convergence in time, as proved in this article. Moreover, the proposed Exponential LRI is about 1000 times more accurate than the semi-implicit Euler method when  $\mu = O(1)$  (similarly as the exponential Euler method in this case), and is more stable than the exponential Euler method when  $\mu \rightarrow 0$  (similarly as the semi-implicit Euler method in this case). Either the exponential Euler method or the semi-implicit Euler method only works well in one of the two cases  $\mu = O(1)$  and  $\mu \rightarrow 1$ , while the proposed Exponential LRI works well for both cases as well as the intermediate case  $\mu = 10^{-2}$ .

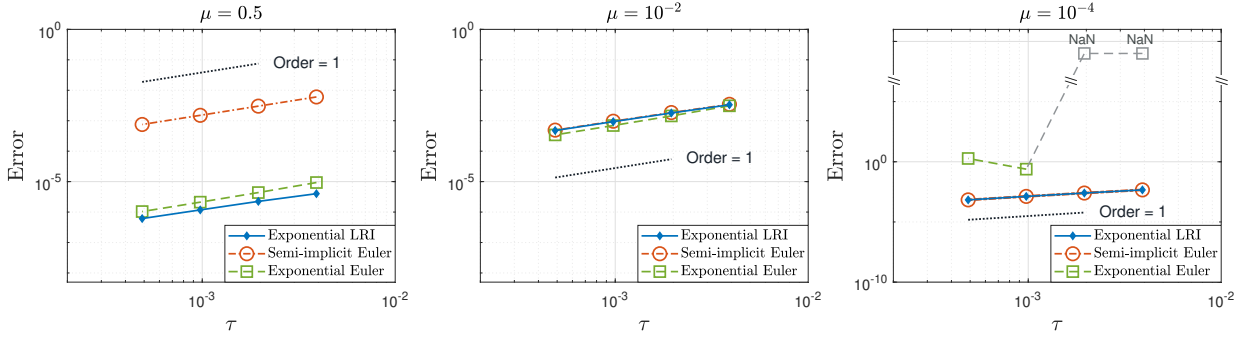


FIGURE 1. Time discretization errors vs stepsizes, with  $H^2$  initial data ( $m = 2.6$ ).

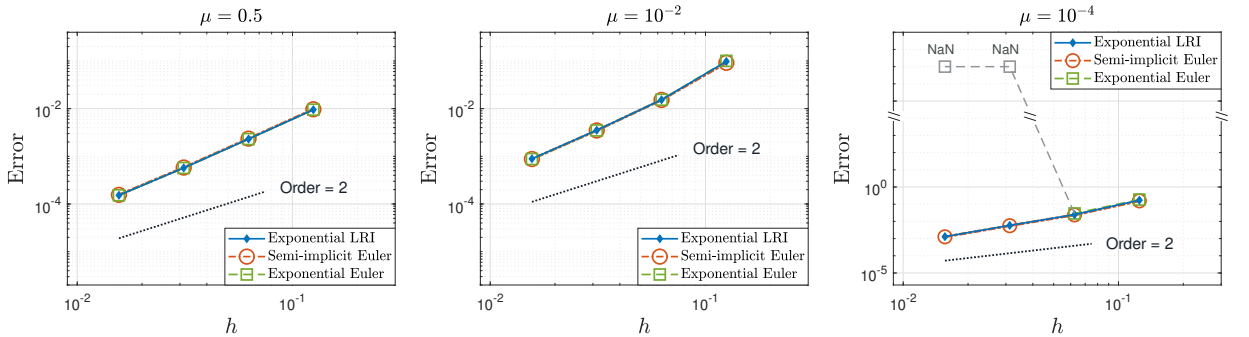


FIGURE 2. Finite element spatial discretization errors vs stepsizes, with  $H^2$  initial data ( $m = 2.6$ ).

The spatial discretization errors by the finite element method is presented in Figure 2, where we see that the spatial discretization has second-order convergence, which is better than the result proved in Theorem 3.1. The rigorous proof of second-order convergence in space is still challenging for this newly proposed method. Moreover, the proposed Exponential LRI is as stable as the semi-implicit Euler method, unlike the exponential Euler method which blows up in the case  $\mu \rightarrow 0$ .

We present the time discretization errors vs CPU time in Figure 3 for the initial value  $u^0 = (u_1^0(x, y), u_2^0(x, y))$  in the domain  $[-\pi, \pi] \times [-\pi, \pi]$  up to time  $T = 1$ , where

$$\begin{aligned} u_1^0(x, y) &= -\frac{m}{2} \cos^m(x/2) \cos^{m-1}(y/2) \sin(y/2), \\ u_2^0(x, y) &= \frac{m}{2} \cos^{m-1}(x/2) \cos^m(y/2) \sin(x/2). \end{aligned}$$

The Fourier collocation method is used for the spatial discretization under the CFL condition  $\tau = 2/M$ , which is used to guarantee the fast convergence of the GMRES solver for the linear systems. We see that the proposed Exponential LRI is about 1000 times more accurate than the semi-implicit Euler method in the case  $\mu = O(1)$  when using the same CPU time (similarly as the exponential Euler method in this case), and is more stable than the exponential Euler method when  $\mu \rightarrow 0$  (similarly as the semi-implicit Euler method in this case). Again, either the exponential Euler method or the semi-implicit Euler method only works well in one of the two cases  $\mu = O(1)$  and  $\mu \rightarrow 1$ , while the proposed Exponential LRI works well for both cases as well as the intermediate case  $\mu = 10^{-2}$ .

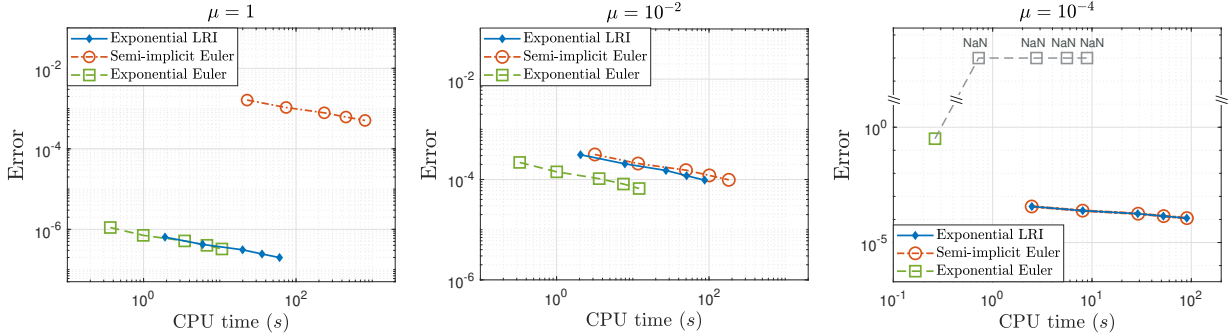
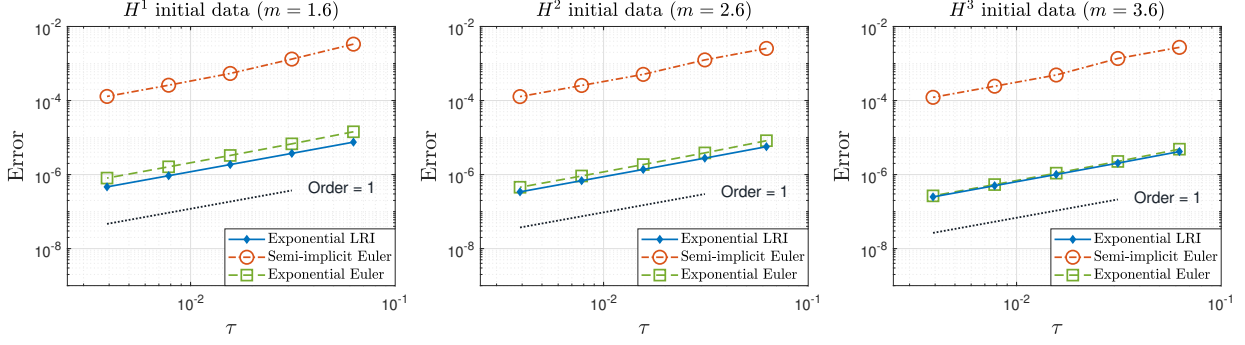
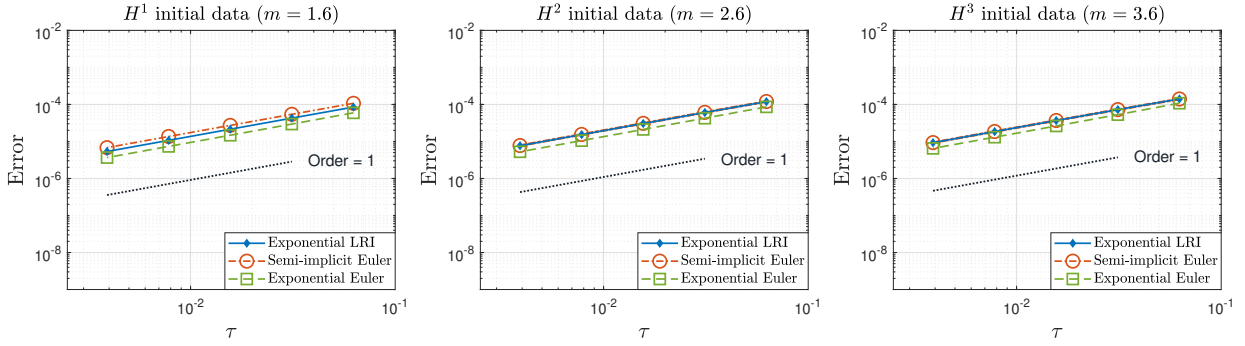
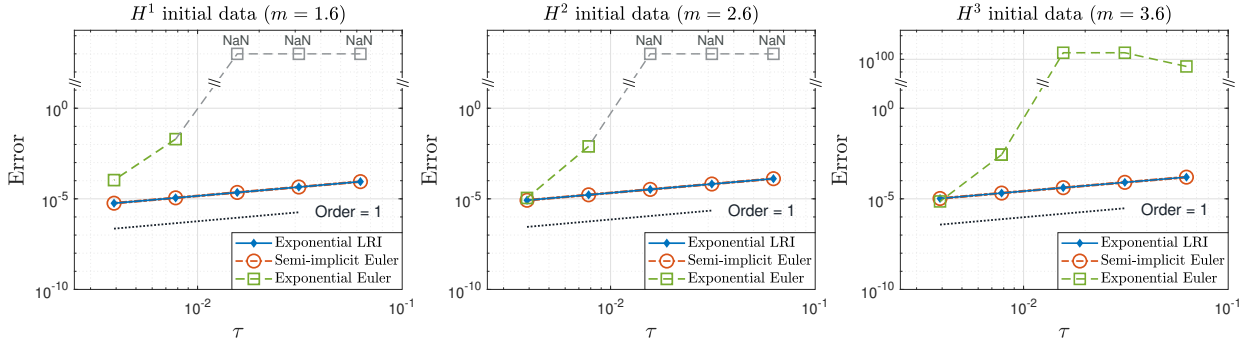


FIGURE 3. Time discretization errors vs CPU time, with the fast Fourier collocation method in space.

The time discretization errors for  $H^1$ ,  $H^2$  and  $H^3$  initial data with Fourier collocation method in space. are presented in Figures 4–6 for the three cases  $\mu = 1$ ,  $\mu = 10^{-2}$  and  $\mu = 10^{-4}$ , respectively. The spatial discretization is performed by the Fourier collocation method with FFT, with a sufficiently large  $M$  so that the spatial discretization errors is negligibly small in observing the temporal discretization errors. From Figures 4–6 we see that the regularity of the initial data does not affect the first-order convergence of the time discretizations. However, the theoretical analysis of first-order convergence for all range of  $\mu$  with initial data below  $H^3$  is still challenging. In this paper, we have set a first step towards weakening the regularity condition of the NS equations for first-order convergence and improving the accuracy of classical methods in both viscous and inviscid cases as well as the intermediate case.

## 5. Conclusions

In this paper we set a first step towards weakening the regularity condition of the NS equations for first-order convergence and improving the accuracy of classical methods in both viscous and inviscid cases. We have proposed a semi-implicit fully discrete low-regularity integrator for the NS equations under both periodic and Dirichlet boundary condition. This

FIGURE 4. Time discretization errors with  $\mu = 1$ .FIGURE 5. Time discretization errors with  $\mu = 0.01$ .FIGURE 6. Time discretization errors with  $\mu = 0.0001$ .

is the first time a low-regularity integrator is coupled with a finite element method in space. The proposed method can be shown to have first-order convergence under weaker regularity conditions than the semi-implicit Euler method and classical exponential integrators. Under periodic boundary conditions, the numerical results show that the proposed method combines the advantages of the semi-implicit Euler method and classical exponential integrator (in both viscous and inviscid cases). In particular, the proposed method is as good as the classical exponential Euler method (much more accurate than the semi-implicit Euler method) in the viscous case  $\mu = O(1)$  when diffusion dominates, and more robust than the classical exponential Euler method in the inviscid case  $\mu \rightarrow 0$  when convection dominates.

In the practical computation, whether diffusion dominates not only depends on the size of  $\mu$  but also depends on other factors, such as the size and shape of domain, and the

largeness of the velocity. It is also possible that convection dominates in one region but diffusion dominates in another region. One advantage of the proposed method, in addition to its theoretical value which weakens the regularity condition for first-order convergence, is that one does not need to distinguish whether diffusion dominates or not, and whether the solution is sufficiently smooth as required by the classical exponential integrator. In either case,  $\mu = O(1)$  or  $\mu \ll 1$ , the proposed method is automatically as good as the better method between the classical exponential integrator and the semi-implicit Euler method.

The semi-implicit exponential low-regularity integrator constructed in this paper is more expensive than typical popular projection methods (for example, see [8, 33, 34]) as it requires the computation of an exponential of the Stokes operator. The development of low-regularity integrators which have similar feature of the projection methods is interesting and challenging. The construction of a low-regularity integrator which allows low regularity approximations and simultaneously resolves the boundary layer effect under the Dirichlet boundary condition in the inviscid case  $\mu \rightarrow 0$  is an interesting and challenging future research direction.

### Acknowledgements

We thank the anonymous referees for their valuable comments and suggestions. K. Schratz has received funding from the European Research Council (ERC) under the European Union's Horizon 2020 research and innovation programme (grant agreement No. 850941). The work of B. Li and S. Ma were supported in part by the Hong Kong Research Grants Council (GRF Project no. 15300519) and the internal grants of The Hong Kong Polytechnic University (Project ID: P0031035 and P0030125, Work programme: ZZKQ and ZZKK).

### Appendix: Fast Fourier transform

For any positive integer  $N$ , we denote by  $I_{2N}$  the  $(4N+1)$ -point trigonometric interpolation operator, which can be obtained through the discrete Fourier transform

$$I_{2N}f(x) = \sum_{k=-2N}^{2N} e^{ikx} \tilde{f}_k \quad \text{with} \quad \tilde{f}_k = \frac{1}{4N+1} \sum_{n=-2N}^{2N} e^{-ikx_n} f(x_n) \quad (\text{A.1})$$

where

$$x_n = \frac{2\pi n}{4N+1} \quad \text{for } n = -2N, \dots, 2N.$$

If the Fourier coefficient  $\hat{f}_k$  of the function  $f$  satisfies that  $\hat{f}_k = 0$  for  $|k| > 2N$ , then  $I_{2N}f = f$  and therefore  $\tilde{f}_k = \hat{f}_k$  in the formula (A.1). In this case, both

$$f(x_n) = \sum_{k=-2N}^{2N} e^{ikx_n} \hat{f}_k, \quad n = -2N, \dots, 2N, \quad (\text{A.2})$$

and

$$\hat{f}_k = \frac{1}{4N+1} \sum_{n=-2N}^{2N} e^{-ikx_n} f(x_n) \quad k = -2N, \dots, 2N,$$

can be computed with cost  $O(N \ln N)$  by using the fast Fourier transform (FFT).

Let  $S_N$  be the subspace of functions  $f \in L^2([0, 2\pi])$  such that  $\hat{f}_k = 0$  for  $|k| > N$ . If  $w, v \in S_N$  and their Fourier coefficients  $\hat{w}_k$  and  $\hat{v}_k$ ,  $k = -2N, \dots, 2N$ , are stored in the computer (with  $\hat{w}_k = \hat{v}_k = 0$  for  $N < |k| \leq 2N$ ), then the values  $w(x_n)$  and  $v(x_n)$ ,  $n = -2N, \dots, 2N$ , can be computed exactly by using (A.2) and FFT. Since  $(\widehat{wv})_k = 0$  for  $|k| > 2N$ , it follows that  $wv = I_{2N}(wv)$ . If we denote by  $\mathcal{F}_k[v]$  the  $k$ th Fourier coefficient of the function  $v$ , then

$$\mathcal{F}_k[wv] = \frac{1}{4N+1} \sum_{n=-2N}^{2N} e^{-ikx_n} w(x_n)v(x_n), \quad k = -2N, \dots, 2N,$$

which can also be computed exactly by using FFT.

## References

- [1] N. Ahmed, T. C. Rebollo, V. John, and S. Rubino. Analysis of a full space-time discretization of the Navier–Stokes equations by a local projection stabilization method. *IMA J. Numer. Anal.*, 37:1437–1467, 2016.
- [2] D. N. Arnold, F. Brezzi, and M. Fortin. A stable finite element for the Stokes equations. *Calcolo*, 21:337–344, 1984.
- [3] R. Bermejo and L. Saavedra. A second order in time local projection stabilized Lagrange–Galerkin method for Navier–Stokes equations at high Reynolds numbers. *Comput. Math. Appl.*, 72:820–845, 2016.
- [4] S. C. Brenner and R. Scott. *The Mathematical Theory of Finite Element Methods*. Texts in Applied Mathematics. Springer-Verlag New York, 3 edition, 2008.
- [5] F. Brezzi and R. Falk. Stability of higher order Taylor–Hood methods. *SIAM J. Numer. Anal.*, 28:581–590, 1991.
- [6] Y. Bruned and K. Schratz. Resonance based schemes for dispersive equations via decorated trees. *Forum of Mathematics, Pi*, 10(article E2), 2022, DOI:10.1017/fmp.2021.13.
- [7] H. Fujita and T. Kato. *On the Navier-Stokes initial value problem I*. *Arch. Rational Mech. Anal.*, 16:269–315, 1964.
- [8] J. L. Guermond, P. Mineev, and J. Shen. An overview of projection methods for incompressible flows. *Comput Methods Appl. Mech. Eng.*, 195:6011–6045, 2006.
- [9] Y. He. The Euler implicit/explicit scheme for the 2D time-dependent Navier–Stokes equations with smooth or non-smooth initial data. *Math. Comp.*, 77:2097–2124, 2008.
- [10] Y. He. The Crank-Nicolson/Adams-Bashforth scheme for the time-dependent Navier-Stokes equations with nonsmooth initial data. *Numer. Methods for PDEs*, 28:155–187, 2011.
- [11] J. G. Heywood and R. Rannacher. Finite element approximation of the nonstationary Navier-Stokes problem IV: Error analysis for second-order time discretization. *SIAM J. Numer. Anal.*, 27:353–384, 1990.
- [12] A. T. Hill and E. Süli. Approximation of the global attractor for the incompressible Navier–Stokes equations. *IMA J. Numer. Anal.*, 20:633–667, 2000.
- [13] M. Hofmanova and K. Schratz. An exponential-type integrator for the KdV equation. *Numer. Math.*, 136:1117–1137, 2017.
- [14] T. Y. Hou. *The nearly singular behavior of the 3D Navier-Stokes equations*. 2021, arXiv:2107.06509.
- [15] R. Ingram. A new linearly extrapolated Crank-Nicolson time-stepping scheme for the Navier-Stokes equations. *Math. Comp.*, 82:1953–1973, 2013.
- [16] D. Jerison and C. E. Kenig. The functional calculus for the Laplacian on Lipschitz domains. *Journées Équations aux dérivées partielles*, pages 1–10, 1989.
- [17] H. Koch and D. Tataru. Well-posedness for the Navier-Stokes equations. *Adv. Math.*, 157:22–35, 2001.
- [18] W. Layton, N. Mays, M. Neda, and C. Trenchea. Numerical analysis of modular regularization methods for the BDF2 time discretization of the Navier-Stokes equations. *ESAIM: M2AN*, 48:765–793, 2014.
- [19] Z. Lei and F. Lin. Global mild solutions of Navier–Stokes equations. *Comm. Pure Appl. Math.*, LXIV:1297–1304, 2011.

- [20] B. Li, S. Ma, and N. Wang. Second-order convergence of the linearly extrapolated Crank–Nicolson method for the Navier–Stokes equations with  $H^1$  initial data. *J. Sci. Comput.*, 88: article 70, 2021.
- [21] B. Li and W. Qiu. A convergent post-processed discontinuous Galerkin method for incompressible flow with variable density. *J. Sci. Comput.*, 91: article 2, 2022.
- [22] B. Li and Y. Wu. A fully discrete low-regularity integrator for the 1D periodic cubic nonlinear Schrödinger equation. *Numer. Math.*, 149:151–183, 2021.
- [23] P. L. Lions. *Mathematical Topics in Fluid Mechanics, Volume 1: Incompressible Models*. Clarendon Press, Oxford, 1996.
- [24] M. López-Fernández. A quadrature based method for evaluating exponential-type functions for exponential methods. *BIT Numer. Math.*, 50:631–655, 2010.
- [25] M. Marion and R. Temam. Navier-Stokes equations: Theory and approximation. *Handbook of numerical analysis*, 6:503–689, 1998.
- [26] R. H. Nochetto and J.-H. Pyo. Error estimates for semi-discrete gauge methods for the Navier–Stokes equations. *Math. Comp.*, 74:521–542, 2016.
- [27] A. Ostermann, F. Rousset, and K. Schratz. Error estimates of a Fourier integrator for the cubic Schrödinger equation at low regularity. *Found. Comput. Math.*, 21:725–765, 2021.
- [28] A. Ostermann, F. Rousset, and K. Schratz. Fourier integrator for periodic NLS: low regularity estimates via discrete Bourgain spaces. To appear in *J. Eur. Math. Soc. (JEMS)*, <https://arxiv.org/abs/2006.12785>.
- [29] A. Ostermann and K. Schratz. Low regularity exponential-type integrators for semilinear Schrödinger equations. *Found. Comput. Math.*, 18:731–755, 2018.
- [30] F. Rousset and K. Schratz. A general framework of low regularity integrators. *SIAM J. Numer. Anal.*, 59:1735–1768, 2021.
- [31] R. S. Saks. Solution of the spectral problem for the curl and Stokes operators with periodic boundary conditions. *Journal of Mathematical Sciences*, 136(2):3794–3811, 2006.
- [32] K. Schratz, Y. Wang, and X. Zhao. Low-regularity integrators for nonlinear Dirac equations. *Math. Comp.*, 90:189–214, 2021.
- [33] J. Shen. On error estimates of projection methods for Navier–Stokes equations: first-order schemes. *SIAM J. Numer. Anal.*, 29:57–77, 1992.
- [34] J. Shen. On error estimates of some higher order projection and penalty-projection methods for Navier–Stokes equations. *Numer. Math.*, 62:49–73, 1992.
- [35] V. Thomée. *Galerkin Finite Element Methods for Parabolic Problems*. Springer-Verlag, New York, second edition, 2006.
- [36] S. Uchiumi. A viscosity-independent error estimate of a pressure-stabilized Lagrange–Galerkin scheme for the Oseen problem. *J. Sci. Comput.*, 80:834–858, 2019.
- [37] E. Wiedemann. *Lecture Notes: Navier–Stokes Equations*. Preprint, Winter 2018.
- [38] Y. Wu and X. Zhao. Embedded exponential-type low-regularity integrators for KdV equation under rough data. *BIT Numer. Math.*, 2021, DOI:10.1007/s10543-021-00895-8.
- [39] Y. Wu and X. Zhao. Optimal convergence of a second order low-regularity integrator for the KdV equation. *IMA J. Numer. Anal.*, 2021, DOI:10.1093/imanum/drab054.

BUYANG LI AND SHU MA: DEPARTMENT OF APPLIED MATHEMATICS, THE HONG KONG POLYTECHNIC UNIVERSITY, HONG KONG. *E-mail address*: [buyang.li@polyu.edu.hk](mailto:buyang.li@polyu.edu.hk) and [maisie.ma@connect.polyu.hk](mailto:maisie.ma@connect.polyu.hk)

KATHARINA SCHRATZ: LABORATOIRE JACQUES-LOUIS LIONS, SORBONNE UNIVERSITÉ, BUREAU : 16-26-315, 4 PLACE JUSSIEU, PARIS 5ÈME. *E-mail address*: [katharina.schratz@sorbonne-universite.fr](mailto:katharina.schratz@sorbonne-universite.fr)